frontiers in Marine Science

ORIGINAL RESEARCH
published: 03 April 2020
doi: 10.3389/fmars.2020.00196

Stripping Voltammetric Determination of Lead in Coastal Waters With a Functional Micro-Needle Electrode

Haitao Han[1,2,3], Dawei Pan[1,2,3], Ying Li[4], Jie Wang[4] and Chenchen Wang[1,2]*

[1] CAS Key Laboratory of Coastal Environmental Processes and Ecological Remediation, Shandong Key Laboratory of Coastal Environmental Processes, Research Center for Coastal Environment Engineering Technology of Shandong Province, Yantai Institute of Coastal Zone Research, Chinese Academy of Sciences, Yantai, China, [2] Center for Ocean Mega-Science, Chinese Academy of Sciences, Qingdao, China, [3] University of Chinese Academy of Sciences, Beijing, China, [4] School of Chemistry and Chemical Engineering, Yantai University, Yantai, China

In this work, for the voltammetric determination of lead (Pb) in coastal waters, a novel functional micro-needle electrode based on 3D reduced graphene oxide/flower-like bismuth nanosheets (3DrGO/F-BiNSs) was fabricated. The micro-needle electrode was prepared with the commercial acupuncture needle (ANE) and functionalized with 3DrGO/F-BiNSs through stepwise electrodeposition method. The sensing surface (needle tip) of the micro-needle electrode was first modified with 3DrGO to enhance the conductivity and provide more active sites to combine Bi nanomaterials. Then the F-BiNSs were electrodeposited on the 3DrGO surface to facilitate the electrochemical voltammetric response of Pb^{2+} due to their excellent combining ability with Pb. The physical and electrochemical properties of the as-prepared 3DrGO/F-BiNSs/ANE were characterized by different techniques including scanning electron microscope (SEM), energy dispersive X-ray spectroscopy (EDS), and electrochemical methods. The 3DrGO/F-BiNSs/ANE exhibited an excellent performance for the voltammetric determination of Pb^{2+} with the linear range of 40 to 600 nmol L^{-1} and detection limit of 12.5 nmol L^{-1}. Additionally, the application of the functional micro-needle electrode for Pb determination in different coastal water samples was also investigated.

Keywords: coastal waters, lead, micro-needle electrode, 3D reduced graphene oxide, flower-like bismuth nanosheets

OPEN ACCESS

Edited by:
Rathinam Arthur James, Bharathidasan University, India

Reviewed by:
Rajkumar Mani, National Environmental Engineering Research Institute, India
Sabarathinam Chidambaram, Kuwait Institute for Scientific Research, Kuwait

***Correspondence:**
Dawei Pan
dwpan@yic.ac.cn

Specialty section:
This article was submitted to Marine Pollution, a section of the journal Frontiers in Marine Science

Received: *26 September 2019*
Accepted: *13 March 2020*
Published: *03 April 2020*

Citation:
Han H, Pan D, Li Y, Wang J and Wang C (2020) Stripping Voltammetric Determination of Lead in Coastal Waters With a Functional Micro-Needle Electrode. Front. Mar. Sci. 7:196. doi: 10.3389/fmars.2020.00196

INTRODUCTION

In the past decades, with the development of global economy and industry, much attention has been attracted to the marine environmental pollution problems. Lead (Pb), one of the heavy metal ions, is highly toxic to the marine aquatic plants and animals and eventually harmful to the human beings through bioaccumulation (Kazi et al., 2009; Chang et al., 2014). It has been reported that the content of Pb in coastal waters is much higher than that in the open ocean because of the enormous amount of anthropogenic contamination (Zhang et al., 2016). Therefore, determination of Pb^{2+} in coastal waters is of great importance for the environmental protection and public health. Many techniques have been developed for the determination of heavy metal ions, including

atomic absorption spectroscopy, atomic emission spectroscopy, and inductively coupled plasma–mass spectrometry (Manivannan and Biju, 2011; Zhu et al., 2017). Although these methods possess various advantages and have been commonly used, the requirement of cumbersome instruments, time-consuming pretreatments, and high cost are the inevitable limitations (Hu et al., 2015; Zhang et al., 2016).

As an efficient electrochemical technique for the determination of heavy metals, anodic stripping voltammetry (ASV) has attracted much attention due to its advantages, such as high sensitivity, rapid response, and straightforward analytical processes (Aragay et al., 2011b; Wang et al., 2014; Lin et al., 2016). In the past decades, mercury electrode, such as hanging mercury electrode, dropping mercury electrode, and mercury film electrode has been commonly adopted for the ASV determination of heavy metals (Nedeltcheva et al., 2005; Annibaldi et al., 2015; Granado-Castro et al., 2018). However, the drawbacks of serious toxicity and difficulties in handling process limited the continued widespread application of mercury electrode (Nagai et al., 2004; Guzzi and La Porta, 2008). After the introduction of bismuth (Bi) film electrode (Wang et al., 2000), Bi-based electrode has been studied in-depth and considered as an attractive alternative to mercury electrode because of its similar property in easy formation of alloys with heavy metals (Wang et al., 2000; Nedeltcheva et al., 2005; Wang, 2005; Saturno et al., 2011). More importantly, Bi-based electrode is much more environmental friendly than mercury electrode.

Graphene (GR) is a planar two-dimensional (2D) honeycomb-like lattice consists of sp2-hybridized carbon atoms monolayer. It has attracted considerable attention as electrode modifier because of its large specific surface area, outstanding electrical conductivity, and excellent electrochemical properties (Brownson and Banks, 2010; Gan and Hu, 2011; Han et al., 2014; Cinti and Arduini, 2017). The three-dimensional (3D) architecture of 2D graphene is an emerging graphene-based nanomaterial which provides a larger electroactive surface area and better opportunity for the loading of functional materials to construct electro-/bio-chemical sensors with excellent sensing performance (Baig and Saleh, 2018). 3D graphene which can be prepared by electrochemical methods has been proved to be a promising and outstanding electrode modifier and ideal platform for the combination of functional materials for electrochemical sensing (Dong et al., 2012; Yang et al., 2015; Baig and Saleh, 2018).

Acupuncture needle (ANE) which has been using for medical therapies originating from China is now a new emerging electrode substrate for the fabrication of novel electrochemical sensors with high sensitivity (Zhou et al., 2017; Han et al., 2018, 2019). In recent years, the micro-needle electrode based on stainless steel ANE has been most widely adopted due to its advantages in flexibility, easy operation, and low price (Tang et al., 2015; Niu et al., 2018). The electrochemical sensing platform based on the micro-needle electrode exhibits much superior performance in the field of electrochemical analysis. Tang et al. (2017) used the unique needle shape of ANE to fabricate a microsensor for real-time monitoring of nitric oxide in acupoints of rats. Li et al. (2019) used the advantage of large specific surface area of ANE to prepare a copper microspheres and polyaniline film modified micro-needle electrode which has good performance for nitrate determination. Han et al. (2019) also used the large specific surface area of ANE and prepared a porous gold modified ANE with excellent performance for copper determination. So, considering the low price, non-toxicity, large specific surface area, and excellent performance of ANE, it was used in this work.

The main aim of this work was to fabricate a novel electrode for the determination of Pb in coastal waters. Based on this, a micro-needle electrode was constructed and functionalized with 3D reduced graphene oxide (3DrGO) and flower-like Bi nanosheets (F-BiNSs). The so-fabricated 3DrGO/F-BiNSs functionalized ANE (3DrGO/F-BiNSs/ANE) exhibited a good performance for the anodic stripping voltammetric determination of Pb^{2+}. Additionally, the practical application of the novel functional micro-needle electrode for Pb^{2+} determination in coastal water samples was conducted with satisfactory results.

MATERIALS AND METHODS

Reagents and Apparatus

The stock standard solution of Pb^{2+} (1000 mg L^{-1}) was purchased from the National Research Centre for Certified Reference Materials (CRMs), Beijing, China. All the other reagents were analytical-grade chemicals and used without further purification. Acetate buffer solutions with pH ranging from 3.0 to 5.0 were prepared by 0.1 mol L^{-1} acetic acid and 0.1 mol L^{-1} sodium acetate. Deionized water (18.2 MΩ cm specific resistance) obtained with a Pall Cascada laboratory water system was used throughout. Graphene oxide (GO) was provided by Nanjing XFNANO Materials Tech Co., Ltd. (Nanjing, China). Acupuncture needles (stainless steel, 0.25 × 60 mm) were provided by Suzhou Medical Appliance Factory Co., Ltd., China. Silicone rubber (NANDA no. 704) was obtained from Liyang Kangda Chemical Co., Ltd., China.

The morphology characterization and element analysis of the bare ANE, 3DrGO modified ANE (3DrGO/ANE) and 3DrGO/F-BiNSs/ANE were conducted on scanning electron microscopy (SEM, Hitachi S-4800 microscope, Japan) and energy dispersive X-ray spectroscopy (EDS, HORIBAEX-350, Japan), respectively. All the electrochemical experiments were performed on a CHI 660E Electrochemical Work Station (CH Instruments, Inc., Shanghai, China) using a conventional three-electrode system. The functional micro-needle electrode was used as the working electrode, with an Ag/AgCl electrode and platinum foil serving as reference and counter electrode, respectively. 797 VA computrace analyzer (Metrohm Ltd., Switzerland) was used for the validation of the values obtained with the 3DrGO/F-BiNSs/ANE. All potentials were measured with respect to the Ag/AgCl reference electrode.

Preparation of the 3DrGO/F-BiNSs/ANE

The fabrication process of the 3DrGO/F-BiNSs/ANE was shown in **Figure 1**. Before modification, the bare micro-needle electrode

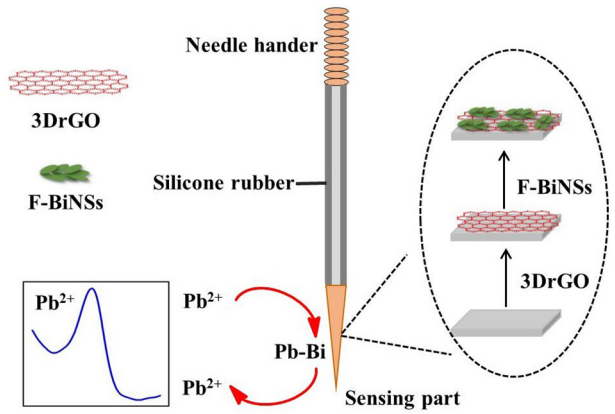

FIGURE 1 | Schematic illustration for the fabrication process of 3DrGO/F-BiNSs/ANE and the detection of Pb^{2+}.

(ANE) was prepared according to our previous work with little modification (Han et al., 2019). Simply, the body part of the ANE was covered with silicone rubber for sealing, leaving the needle tip (about 1 mm) as sensing surface and the needle handle as electrode wire. The modification of ANE with 3DrGO was conducted by cycling the potentials from 0.5 to −1.5 V in 0.5 mg L^{-1} GO solution for 30 circles with ANE as the working electrode (Baig and Saleh, 2018). The 3DrGO/F-BiNSs/ANE was prepared by electrodepositing at −0.6 V in 0.5 mmol L^{-1} $Bi(NO_3)_3$ solution for 60 s with 3DrGO/ANE as the working electrode. The functional micro-needle electrode was obtained eventually after the cleaning and drying processes at room temperature.

Electrochemical Analysis Procedures

Unless otherwise stated, 0.1 mol L^{-1} acetate buffer solution was adopted as the supporting electrolyte for the determination of Pb^{2+}. Quantitative determination of Pb^{2+} was performed with square wave voltammetry (SWV) from −0.65 to −0.4 V (−0.8 to −0.3 V for the determination of Pb in coastal water samples) by using the following parameters: accumulation potential of −0.75 V, accumulation time of 240 s, amplitude of 0.025 V, potential incremental of 0.004 V, frequency of 25 Hz, and quiet time of 2 s. After one measurement, a cleaning process was applied to the electrode at −0.4 V for 30 s with stirring. The standard addition method was adopted for the determination of Pb^{2+} in coastal water samples. The electrochemical impedance spectroscopy (EIS) of different modified micro-needle electrodes was conducted in 5 mmol L^{-1} $K^3[Fe(CN)^6]$ (0.1 mol L^{-1} KCl) solution with the frequency ranging from 10^{-2} to 10^5 Hz.

Stability, Repeatability and Selectivity

The stability of the functional micro-needle electrode was evaluated by determining 1 μmol L^{-1} Pb^{2+} at the same 3DrGO/F-BiNSs/ANE for six measurements. The reproducibility was investigated by determining 1 μmol L^{-1} Pb^{2+} at six independently fabricated 3DrGO/F-BiNSs/ANEs. The selectivity was evaluated by the influence of different potential foreign ions (K^+, Na^+, Ca^{2+}, Mg^{2+}, Cr^{3+}, NO_3^-, SO_4^{2-}, Cl^-, Co^{2+}, Cd^{2+}, Cu^{2+}) on the electrochemical response of Pb^{2+} at the 3DrGO/F-BiNSs/ANE. Current responses of 1 μmol L^{-1} Pb^{2+} were obtained after the addition of different foreign species into acetate buffer solution under the optimal conditions.

Preparation of Coastal Water Samples

The coastal water samples were collected from the Yuniao River Estuary (Shandong Province, China) at different locations. All the water samples were filtered with 0.45 μm membrane filters and kept in the fridge (4°C) until determination. Before determination with standard addition method, the samples were adjusted to pH 3.5 by using 0.4 mol L^{-1} acetic acid solutions.

RESULTS AND DISCUSSION

Characterization of the 3DrGO/F-BiNSs/ANE

The morphologies of different modified micro-needle electrodes were investigated by SEM (**Figure 2**). The SEM image of the so-prepared bare ANE and its low magnification image (the insert) were showed in **Figure 2A**. It can be seen that the surface of the bare ANE was very smooth which provided limited binding sites for the combination of functional nanomaterials. The diameter of the needle tip was around 5 μm as described in our previous publications (Han et al., 2018, 2019). **Figure 2B** showed the SEM image of the surface of 3DrGO modified ANE which exhibited an interconnected 3D network of rGO sheets. The morphology was consistent with the 3D graphene synthesized and reported in the previous publication (Cui et al., 2013). The 3D graphene network provided larger exposed surface area and more active sites which were helpful for the direct electron transfer and combination of functional nanomaterials. After the process of electrochemical

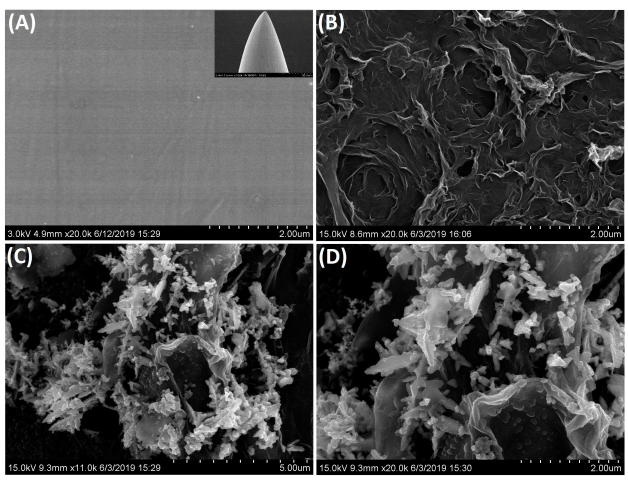

FIGURE 2 | SEM images of the bare ANE **(A)**, 3DrGO/ANE **(B)**, and 3DrGO/F-BiNSs/ANE **(C,D)**. Inset in **(A)** shows the low magnification of bare ANE.

deposition in $Bi(NO_3)_3$ solution, Bi nanosheets with flower-like structure were distributed on the surface of 3DrGO (**Figures 2C,D**). From the SEM characterization, it can be concluded that all the 3DrGO and F-BiNSs could be modified on the micro-needle electrode by the electrodeposition method. The novel functional micro-needle electrode exhibited a good performance for the voltammetric determination of Pb^{2+} as discussed below.

To investigate the elemental composition of different modified micro-needle electrodes, EDS was conducted (**Figure 3**). It can be seen clearly that Fe, Cr, Ni, C, and Si were the main elements of the stainless steel ANE. When compared with the bare ANE, the content percentage of C increased obviously in the 3DrGO/ANE, which might be caused by the presence of 3DrGO. After the electrochemical deposition of F-BiNSs on 3DrGO/ANE, the typical Bi peaks at about 2.42, 9.45, and 10.81 KeV appeared on the EDS pattern of 3DrGO/F-BiNSs/ANE, which proved the presence of F-BiNSs. It can be concluded from the results of SEM and EDS characterizations that the functional micro-needle electrode, 3DrGO/F-BiNSs/ANE, was successfully fabricated.

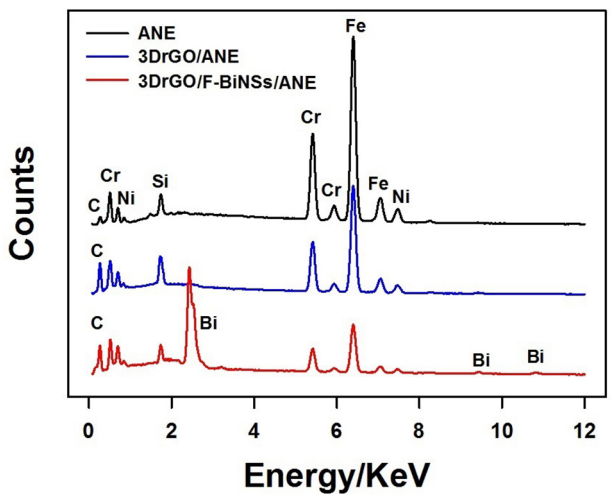

FIGURE 3 | EDS spectra of the bare ANE, 3DrGO/ANE, and 3DrGO/F-BiNSs/ANE.

Cyclic voltammetry (CV) and linear sweep voltammetry (LSV) were used to investigate the electrochemical properties of the functional micro-needle electrode. The cyclic voltammograms of different electrodes were recorded from −0.4 to 0.6 V in acetate buffer solution (**Figure 4A**). There was no peak could be observed in the cyclic voltammograms of bare ANE and 3DrGO/ANE. However, the background current of 3DrGO/ANE was much higher than that of bare ANE, which proved the excellent conductivity of 3DrGO. After the electrodeposition of F-BiNSs, the 3DrGO/F-BiNSs/ANE exhibited a sharp typical oxidation peak of Bi at 0.08 V. The results of LSV were similar with that of CV, and there was almost no difference between ANE and 3DrGO/ANE (**Figure 4B**). However, the oxidation peak of Bi at 0.16 V appeared on the 3DrGO/F-BiNSs/ANE. So, the 3DrGO and F-BiNSs could be modified on the ANE by electrodeposition method and the F-BiNSs might be stripped out when the potential exceeded 0.08 V.

Electrochemical impedance spectroscopy was conducted in $K_3[Fe(CN)_6]$ solution to investigate the electron transfer capability of different micro-needle electrodes (**Figure 5**). It is known that the charge transfer resistance (Rct) can be reflected by the semicircle diameter of Nyquist plot at high frequency part. It can be observed that the semicircle diameter of 3DrGO/ANE was much smaller than that of bare ANE which reflected the excellent conductivity of 3DrGO. However, after the modification of F-BiNSs, the Rct became relatively larger than that of 3DrGO/ANE. It was obvious that the electro-conductivity of F-BiNSs was relatively weaker than that of 3DrGO. Despite its relatively weak conductivity, F-BiNSs

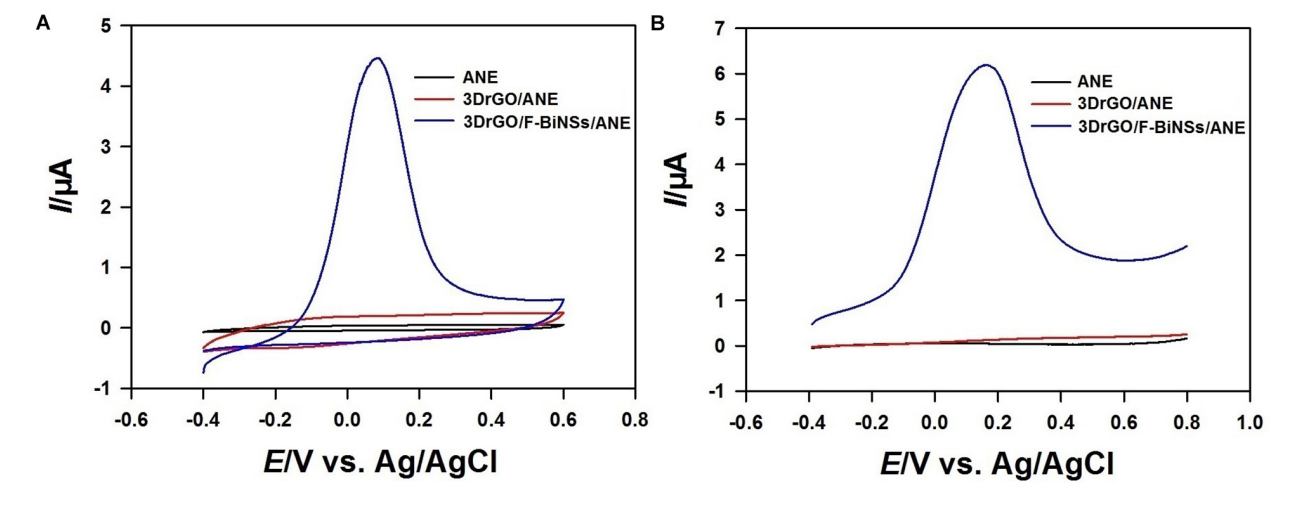

FIGURE 4 | Cyclic voltammograms **(A)** and linear sweep voltammograms **(B)** of the bare ANE, 3DrGO/ANE, and 3DrGO/F-BiNSs/ANE in 0.1 mol L^{-1} acetate buffer solution with the scan rate of 50 mV s^{-1}.

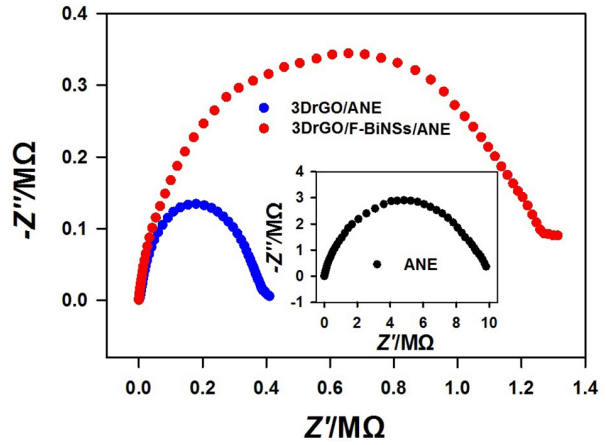

FIGURE 5 | Nyquist plots of the bare ANE, 3DrGO/ANE, and 3DrGO/F-BiNSs/ANE in 5 mmol L^{-1} $K_3[Fe(CN)_6]$ solution (0.1 mol L^{-1} KCl).

enhanced the electrochemical sensing performance of the micro-needle electrode for Pb^{2+} as discussed below due to their excellent property in easy formation of alloys with heavy metals.

Electrochemical Response of Lead on the 3DrGO/F-BiNSs/ANE

The electrochemical responses of Pb^{2+} on different micro-needle electrodes were also investigated by using SWV (**Figure 6**). The bare ANE and 3DrGO/ANE had no obvious current response to 1 μmol L^{-1} Pb^{2+}. So, there was no obvious enhancement for Pb^{2+} determination when 3DrGO was modified on the micro-needle electrode. However, it provided larger exposed surface area and more active sites for the combination of Bi nanomaterials which could enhance the electrochemical voltammetric responses of Pb^{2+} significantly. As expected,

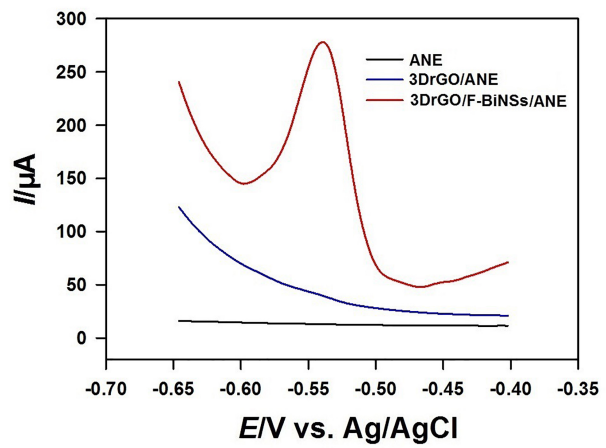

FIGURE 6 | Square wave voltammograms of the bare ANE, 3DrGO/ANE, and 3DrGO/F-BiNSs/ANE in 0.1 mol L^{-1} acetate buffer (pH 3.5) solution containing 1 μmol L^{-1} Pb^{2+}.

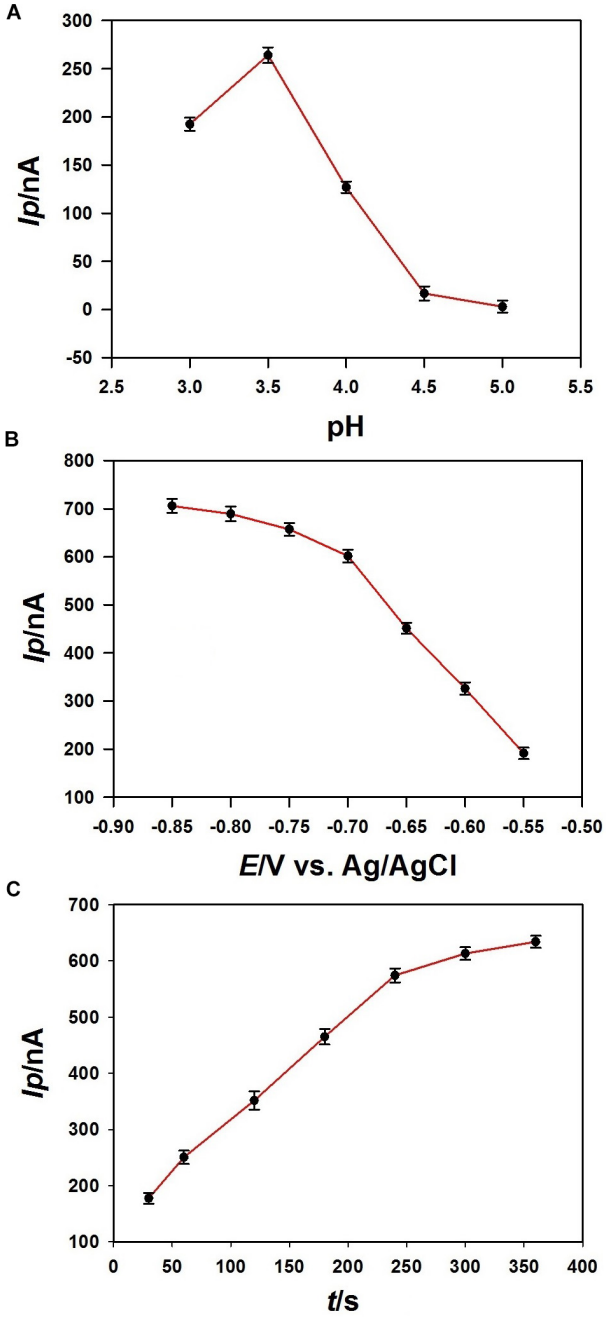

FIGURE 7 | Effects of pH **(A)**, accumulation potential **(B)**, and accumulation time **(C)** on the peak current (Ip) of 1 μmol L^{-1} Pb^{2+} (n = 3) obtained at the 3DrGO/F-BiNSs/ANE.

a large oxidation peak at about −0.54 V appeared on the voltammogram of 3DrGO/F-BiNSs/ANE. It was obvious that the 3DrGO/F-BiNSs/ANE showed an enhanced performance for the voltammetric determination of Pb^{2+} due to the combining ability of F-BiNSs with heavy metals (Pb here) and the 3D structure and excellent conductivity of 3DrGO.

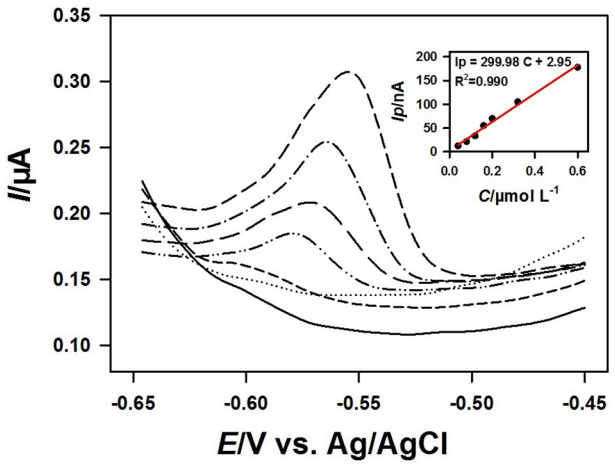

FIGURE 8 | Square wave voltammograms obtained at the 3DrGO/F-BiNSs/ANE with successive addition of 0.04, 0.08, 0.12, 0.16, 0.20, 0.32, 0.60 μmol L^{-1} Pb^{2+} in 0.1 mol L^{-1} acetate buffer (pH 3.5). Inset shows the corresponding calibration curve of Pb^{2+} from 0.04 to 0.60 μmol L^{-1} (n = 3) at the 3DrGO/F-BiNSs/ANE.

Optimization for Pb Response on the 3DrGO/F-BiNSs/ANE

The effect of pH value of the acetate buffer for the stripping voltammetric determination of Pb^{2+} on the 3DrGO/F-BiNSs/ANE was investigated (**Figure 7A**). Stripping peak current (Ip) was obtained for 1 μmol L^{-1} Pb^{2+} determination with the pH value ranging from 3.0 to 5.0. It can be seen that the maximum oxidation Ip appeared at pH 3.5 and decreases when the pH increased from 3.5 to 5.0. As reported, the decrease of Ip at pH higher than 3.5 might be explained as the hydrolysis of Pb^{2+} (Wang et al., 2019). As a result, a pH of 3.5 was selected and used for the voltammetric determination of Pb^{2+} in this work.

It is known that the accumulation potential has significant effect on the stripping voltammetric responses of metal ions. The effect of accumulation potential on the Ip of 1 μmol L^{-1} Pb^{2+} obtained with the 3DrGO/F-BiNSs/ANE was investigated with the potential varying from −0.55 to −0.85 V (**Figure 7B**). It can be seen that the Ip increased continuously with the potential from −0.55 to −0.85 V. More Pb^{2+} could be reduced and accumulated on the electrode surface by the more negative potentials in this process, which led to the stronger current response. Though a more negative potential could increase the accumulation amount of Pb^{2+} and improve the sensitivity, it also enhanced the noise current of the micro-needle electrode. So, −0.75 V was selected as the accumulation potential and used throughout the work.

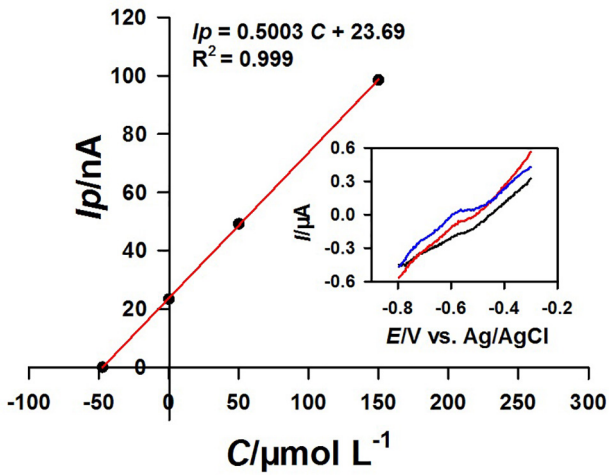

FIGURE 9 | Typical linear regression for the determination of Pb^{2+} (n = 3) in coastal water samples at 3DrGO/F-BiNSs/ANE by the standard addition method and corresponding square wave voltammograms obtained with 0, 50, and 150 nmol L^{-1} Pb^{2+} added.

TABLE 2 | Results of Pb^{2+} determination in real coastal water samples (n = 3) obtained with the 3DrGO/F-BiNSs/ANE.

Coastal water samples	Pb^{2+} added/ μmol L^{-1}	Pb^{2+} determined/ μmol L^{-1}	Recovery (%)
Estuarine water 1	0	0.047	–
Estuarine water 2	0	0.426	–
Coastal river water	0	0.585	–
	0.5	1.113	102.6
	1	1.542	97.3

TABLE 1 | Comparison of the 3DrGO/F-BiNSs/ANE with other modified electrodes for the determination of Pb^{2+}.

Electrode	Method	Linear range/μmol L^{-1}	Detection limit/μmol L^{-1}	References
FGO/GCE	SWV	0.3–5	0.01	Thiruppathi et al., 2017
Nafion-HAP/GCE	DPV	0.1–10.0	0.049	Gao et al., 2016
MPCS-CO-Cys-GCE	SWV	0.1–0.8	0.1	Zhang et al., 2012
PANI/GCE	SWV	0–2	0.1	Wang et al., 2011
PEDOT/SDS/GCE	SWV	0.048–0.965	0.034	Vedhi et al., 2008
Bi/PANI/GCE	SWV	0.025–0.15	0.0165	Wang et al., 2010
CNP/SPE	SWV	0.024–0.193	–	Aragay et al., 2011a
3DrGO/F-BiNSs/ANE	SWV	0.04–0.6	0.0125	This work

FGO, fluorinated graphene oxide; GCE, glassy carbon electrode; Nafion-HAP, Nafion-hydroxyapatite; MPCS-CO-Cys, cysteine-modified three dimensional macroporous carbon spheres; PANI, polyaniline; PEDOT/SDS, poly(3,4-ethylenedioxythiophene)/sodium dodecyl sulfate; CNP, carbon nanoparticles; SPE, screen printed electrode; DPV, differential pulse voltammetry.

The effect of accumulation time on the current response was also investigated with the time ranging from 30 to 360 s when the deposition potential was fixed at −0.75 V (**Figure 7C**). It can be seen that although the Ip increased continuously with the accumulation time ranging from 30 to 360 s, the increasing trend slowed down after the time reaching to 240 s. So, in this work, 240 s was adopted as the accumulation time for the determination of Pb^{2+} in coastal water samples. Additionally, a prolonged accumulation time could be selected for the determination of Pb^{2+} with lower concentration.

Performance Evaluation of the 3DrGO/F-BiNSs/ANE

Figure 8 showed the square wave voltammograms and the corresponding calibration curve of different concentrations of Pb^{2+} on the 3DrGO/F-BiNSs/ANE under the optimal conditions. The Ip was linear with the concentration of Pb^{2+} ranging from 40 to 600 nmol L^{-1} with the equation for linear regression Ip = 299.98 C + 2.95 (R^2 = 0.990). The detection limit (LOD) of the 3DrGO/F-BiNSs/ANE for the voltammetric determination of Pb^{2+} was calculated as 12.5 nmol L^{-1}. It should be noted that the detection performance could be enhanced by adjusting the accumulation potential and time as described above. Additionally, the comparison of the functional micro-needle electrode with other modified electrodes for the determination of Pb^{2+} was presented in **Table 1**. When compared with the modified electrodes developed previously, the newly fabricated 3DrGO/F-BiNSs/ANE showed a satisfactory performance for the voltammetric determination of Pb^{2+}. Furthermore, the 3DrGO/F-BiNSs/ANE exhibited good stability, repeatability and selectivity for the voltammetric determination of Pb^{2+}. The relative standard deviation (RSD) of six determinations of 1 μmol L^{-1} Pb^{2+} at the same 3DrGO/F-BiNSs/ANE was calculated as 3.8%. The RSD of six independently fabricated 3DrGO/F-BiNSs/ANEs for the determination of 1 μmol L^{-1} Pb^{2+} was 5.2%. The results of selectivity evaluation showed that 100-fold K^+, Na^+, Ca^{2+}, Mg^{2+}, Cr^{3+}, NO_3^-, SO_4^{2-}, Cl^-, 50-fold Zn^{2+}, 20-fold Co^{2+}, Cd^{2+}, and 10-fold Cu^{2+} had no obvious effect on the voltammetric determination of Pb^{2+} (<5% current change). Therefore the functional micro-needle electrode might be a good choice for the determination of Pb^{2+}.

Determination of Pb^{2+} in Coastal Waters With the 3DrGO/F-BiNSs/ANE

The practical application of the functional micro-needle electrode for the determination of Pb^{2+} in real coastal water samples was also evaluated. **Figure 9** showed the typical linear regression and corresponding square wave voltammograms obtained after the successive addition of 0, 50, and 150 nmol L^{-1} Pb^{2+}. The Pb^{2+} concentration in this coastal water sample was calculated to be 47.3 nmol L^{-1}. The Pb^{2+} concentrations of different coastal water samples and corresponding recoveries were presented in **Table 2**. For comparison, the coastal water samples were also determined with the common mercury electrode via Metrohm 797 VA computrace analyzer (Zhao et al., 2019). The results obtained by these two methods were consistent. The results showed that the 3DrGO/F-BiNSs/ANE fabricated here could be used for the voltammetric determination of Pb^{2+} in fresh and brackish water samples.

CONCLUSION

This work described a new method for the determination of Pb in coastal waters with a cheap and non-toxic functional micro-needle electrode. The detection performance of the micro-needle electrode was significantly enhanced by the 3DrGO/F-BiNSs. The newly fabricated 3DrGO/F-BiNSs/ANE exhibited a good performance for the voltammetric determination of Pb^{2+}. The practical application of the functional micro-needle electrode for Pb determination in coastal water samples was conducted. Furthermore, the distribution of Pb in coastal waters of different regions could be investigated with the functional micro-needle electrode in the future.

DATA AVAILABILITY STATEMENT

All datasets generated for this study are included in the article/supplementary material.

AUTHOR CONTRIBUTIONS

HH and DP designed the experiments and wrote the manuscript. YL, JW, and CW sampled the coastal waters. HH performed the experiments and analyses.

FUNDING

This work was financially supported by the Key Research and Development Plan of Yantai City (2018ZHGY076), the National Key Research and Development Program of China (2019YFD0901103), the STS Project of Chinese Academy of Sciences (KFJ-STS-ZDTP-023), the Key Research and Development Plan of Shandong Province (2017GHY215002), and the Senior User Project of RV KEXUE (KEXUE2018G04).

ACKNOWLEDGMENTS

We would like to thank Dr. Wenhai Wang for the SEM and EDS characterizations of the modified electrodes.

REFERENCES

Annibaldi, A., Illuminati, S., Truzzi, C., Libani, G., and Scarponi, G. (2015). Pb, Cu and Cd distribution in five estuary systems of Marche, central Italy. *Mar. Pollut. Bull.* 96, 441–449. doi: 10.1016/j.marpolbul.2015.05.008

Aragay, G., Pons, J., and Merkoçi, A. (2011a). Enhanced electrochemical detection of heavy metals at heated graphite nanoparticle-based screen-printed electrodes. *J. Mater. Chem.* 21, 4326–4331. doi: 10.1039/c0jm03751f

Aragay, G., Pons, J., and Merkoçi, A. (2011b). Recent trends in macro-, micro-, and nanomaterial-based tools and strategies for heavy-metal detection. *Chem. Rev.* 111, 3433–3458. doi: 10.1021/cr100383r

Baig, N., and Saleh, T. A. (2018). Electrodes modified with 3D graphene composites: a review on methods for preparation, properties and sensing applications. *Microchim. Acta* 185:283. doi: 10.1007/s00604-018-2809-3

Brownson, D. A. C., and Banks, C. E. (2010). Graphene electrochemistry: an overview of potential applications. *Analyst* 135, 2768–2778. doi: 10.1039/c0an00590h

Chang, J., Zhou, G., Christensen, E. R., Heideman, R., and Chen, J. (2014). Graphene-based sensors for detection of heavy metals in water: a review. *Anal. Bioanal. Chem.* 406, 3957–3975. doi: 10.1007/s00216-014-7804-x

Cinti, S., and Arduini, F. (2017). Graphene-based screen-printed electrochemical (bio)sensors and their applications: efforts and criticisms. *Biosens. Bioelectron.* 89, 107–122. doi: 10.1016/j.bios.2016.07.005

Cui, M., Xu, B., Hu, C., Shao, H. B., and Qu, L. (2013). Direct electrochemistry and electrocatalysis of glucose oxidase on three-dimensional interpenetrating, porous graphene modified electrode. *Electrochim. Acta* 98, 48–53. doi: 10.1016/j.electacta.2013.03.040

Dong, X., Cao, Y., Wang, J., Chan-Park, M. B., Wang, L., Huang, W., et al. (2012). Hybrid structure of zinc oxide nanorods and three dimensional graphene foam for supercapacitor and electrochemical sensor applications. *RSC Adv.* 2, 4364. doi: 10.1039/c2ra01295b

Gan, T., and Hu, S. (2011). Electrochemical sensors based on graphene materials. *Microchim. Acta* 175, 1–19. doi: 10.1007/s00604-011-0639-7

Gao, F., Gao, N., Nishitani, A., and Tanaka, H. (2016). Rod-like hydroxyapatite and Nafion nanocomposite as an electrochemical matrix for simultaneous and sensitive detection of Hg^{2+}, Cu^{2+}, Pb^{2+} and Cd^{2+}. *J. Electroanal. Chem.* 775, 212–218. doi: 10.1016/j.jelechem.2016.05.032

Granado-Castro, M. D., Casanueva-Marenco, M. J., Galindo-Riaño, M. D., El Mai, H., and Díaz-de-Alba, M. (2018). A separation and preconcentration process for metal speciation using a liquid membrane: a case study for iron speciation in seawater. *Mar. Chem.* 198, 56–63. doi: 10.1016/j.marchem.2017.11.009

Guzzi, G., and La Porta, C. A. M. (2008). Molecular mechanisms triggered by mercury. *Toxicology* 244, 1–12. doi: 10.1016/j.tox.2007.11.002

Han, H., Li, Y., Pan, D., Wang, C., Pan, F., and Ding, X. (2019). A novel stainless steel needle electrode based on porous gold nanomaterials for the determination of copper in seawater. *Anal. Methods* 11, 1976–1983. doi: 10.1039/c9ay00222g

Han, H., Pan, D., Wu, X., Zhang, Q., and Zhang, H. (2014). Synthesis of graphene/methylene blue/gold nanoparticles composites based on simultaneous green reduction, in situ growth and self-catalysis. *J. Mater. Sci.* 49, 4796–4806. doi: 10.1007/s10853-014-8179-2

Han, H., Tao, W., Hu, X., Ding, X., Pan, D., Wang, C., et al. (2018). Needle-shaped electrode for speciation analysis of copper in seawater. *Electrochim. Acta* 289, 474–482. doi: 10.1016/j.electacta.2018.08.097

Hu, X., Pan, D., Lin, M., Han, H., and Li, F. (2015). One-step electrochemical deposition of reduced graphene oxide-bismuth nanocomposites for determination of lead. *ECS Electrochem. Lett.* 4, H43–H45. doi: 10.1149/2.0021509eel

Kazi, T. G., Jamali, M. K., Arain, M. B., Afridi, H. I., Jalbani, N., Sarfraz, R. A., et al. (2009). Evaluation of an ultrasonic acid digestion procedure for total heavy metals determination in environmental and biological samples. *J. Hazard. Mater.* 161, 1391–1398. doi: 10.1016/j.jhazmat.2008.04.103

Li, Y., Han, H., Pan, D., and Zhang, P. (2019). Fabrication of a micro-needle sensor based on copper microspheres and polyaniline film for nitrate determination in coastal river waters. *J. Electrochem. Soc.* 166, B1038–B1043. doi: 10.1149/2.1281912jes

Lin, M., Pan, D., Zhu, Y., Hu, X., Han, H., and Wang, C. (2016). Dual-nanomaterial based electrode for voltammetric stripping of trace Fe(II) in coastal waters. *Talanta* 154, 127–133. doi: 10.1016/j.talanta.2016.03.060

Manivannan, D., and Biju, V. M. (2011). Determination of toxic heavy metals in sea water by FAAS after preconcentration with a novel chelating resin. *Water Sci. Technol.* 64, 803–808. doi: 10.2166/wst.2011.501

Nagai, T., Imai, A., Matsushige, K., Yokoi, K., and Fukushima, T. (2004). Voltammetric determination of dissolved iron and its speciation in freshwater. *Limnology* 5, 87–94. doi: 10.1007/s10201-004-0121-x

Nedeltcheva, T., Atanassova, M., Dimitrov, J., and Stanislavova, L. (2005). Determination of mobile form contents of Zn, Cd, Pb and Cu in soil extracts by combined stripping voltammetry. *Anal. Chim. Acta* 528, 143–146. doi: 10.1016/j.aca.2004.10.036

Niu, X., Wen, Z., Li, X., Zhao, W., Li, X., Huang, Y., et al. (2018). Fabrication of graphene and gold nanoparticle modified acupuncture needle electrode and its application in rutin analysis. *Sens. Actuators B Chem.* 255, 471–477. doi: 10.1016/j.snb.2017.07.085

Saturno, J., Valera, D., Carrero, H., and Fernández, L. (2011). Electroanalytical detection of Pb, Cd and traces of Cr at micro/nano-structured bismuth film electrodes. *Sens. Actuators B Chem.* 159, 92–96. doi: 10.1016/j.snb.2011.06.055

Tang, L., Du, D., Yang, F., Liang, Z., Ning, Y., Wang, H., et al. (2015). Preparation of graphene-modified acupuncture needle and its application in detecting neurotransmitters. *Sci. Rep.* 5:11627. doi: 10.1038/srep11627

Tang, L., Li, Y., Xie, H., Shu, Q., Yang, F., Liu, Y.-L., et al. (2017). A sensitive acupuncture needle microsensor for real-time monitoring of nitric oxide in acupoints of rats. *Sci. Rep.* 7:6446. doi: 10.1038/s41598-017-06657-3

Thiruppathi, A. R., Sidhureddy, B., Keeler, W., and Chen, A. (2017). Facile one-pot synthesis of fluorinated graphene oxide for electrochemical sensing of heavy metal ions. *Electrochem. Commun.* 76, 42–46. doi: 10.1016/j.elecom.2017.01.015

Vedhi, C., Selvanathan, G., Arumugam, P., and Manisankar, P. (2008). Electrochemical sensors of heavy metals using novel polymer-modified glassy carbon electrodes. *Ionics* 15, 377–383. doi: 10.1007/s11581-008-0277-1

Wang, J. (2005). Stripping analysis at bismuth electrodes: a review. *Electroanalysis* 17, 1341–1346. doi: 10.1002/elan.200403270

Wang, J., Lu, J., Hocevar, S. B., and Farias, P. A. M. (2000). Bismuth-coated carbon electrodes for anodic stripping voltammetry. *Anal. Chem.* 72, 3218–3222. doi: 10.1021/ac000108x

Wang, R., Ji, W., Huang, L., Guo, L., and Wang, X. (2019). Electrochemical determination of lead(II) in environmental waters using a sulfydryl modified covalent organic framework by square wave anodic stripping voltammetry (SWASV). *Anal. Lett.* 52, 1757–1770. doi: 10.1080/00032719.2019.1568448

Wang, Z., Liu, E., and Zhao, X. (2011). Glassy carbon electrode modified by conductive polyaniline coating for determination of trace lead and cadmium ions in acetate buffer solution. *Thin Solid Films* 519, 5285–5289. doi: 10.1016/j.tsf.2011.01.176

Wang, Z., Wang, H., Zhang, Z., and Liu, G. (2014). Electrochemical determination of lead and cadmium in rice by a disposable bismuth/electrochemically reduced graphene/ionic liquid composite modified screen-printed electrode. *Sens. Actuators B Chem.* 199, 7–14. doi: 10.1016/j.snb.2014.03.092

Wang, Z. M., Guo, H. W., Liu, E., Yang, G. C., and Khun, N. W. (2010). Bismuth/polyaniline/glassy carbon electrodes prepared with different protocols for stripping voltammetric determination of trace Cd and Pb in solutions having surfactants. *Electroanalysis* 22, 209–215. doi: 10.1002/elan.200900251

Yang, Y., Kang, M., Fang, S., Wang, M., He, L., Zhao, J., et al. (2015). Electrochemical biosensor based on three-dimensional reduced graphene oxide and polyaniline nanocomposite for selective detection of mercury ions. *Sens. Actuators B Chem.* 214, 63–69. doi: 10.1016/j.snb.2015.02.127

Zhang, X., Zhang, Y., Ding, D., Zhao, J., Liu, J., Yang, W., et al. (2016). On-site determination of Pb^{2+} and Cd^{2+} in seawater by double stripping voltammetry with bismuth-modified working electrodes. *Microchem. J.* 126, 280–286. doi: 10.1016/j.microc.2015.12.010

Zhang, Y., Zhang, J., Liu, Y., Huang, H., and Kang, Z. (2012). Highly ordered three-dimensional macroporous carbon spheres for determination of heavy metal ions. *Mater. Res. Bull.* 47, 1034–1039. doi: 10.1016/j.materresbull.2011.12.051

Zhao, G., Liang, R., Wang, F., Ding, J., and Qin, W. (2019). An all-solid-state potentiometric microelectrode for detection of copper in coastal sediment

pore water. *Sens. Actuators B Chem.* 279, 369–373. doi: 10.1016/j.snb.2018.09.125

Zhou, J.-X., Tang, L.-N., Yang, F., Liang, F.-X., Wang, H., Li, Y.-T., et al. (2017). MoS_2/Pt nanocomposite-functionalized microneedle for real-time monitoring of hydrogen peroxide release from living cells. *Analyst* 142, 4322–4329. doi: 10.1039/c7an01446e

Zhu, X., Zhang, R., Liu, S., Wu, Y., Jiang, Z., and Zhang, J. (2017). Seasonal distribution of dissolved iron in the surface water of Sanggou Bay, a typical aquaculture area in China. *Mar. Chem.* 189, 1–9. doi: 10.1016/j.marchem.2016.12.004

Conflict of Interest: The authors declare that the research was conducted in the absence of any commercial or financial relationships that could be construed as a potential conflict of interest.